DOI 10.5012/bkcs.2011.32.6.2003

Selective Trace Analysis of Mercury (II) Ions in Aqueous Media Using SERS-Based Aptamer Sensor

Chankil Lee and Jaebum Choo[†,*]

Department of Electronics & Communication Engineering, Hanyang University, Ansan 426-791, Korea
[†]Department of Bionano Engineering, Hanyang University, Ansan 426-791, Korea. [*]E-mail: jbchoo@hanyang.ac.kr
Received May 2, 2011, Accepted May 19, 2011

We report a highly sensitive surface-enhanced Raman scattering (SERS) platform for the selective trace analysis of mercury (II) ions in drinkable water using aptamer-conjugated silver nanoparticles. Here, an aptamer designed to specifically bind to Hg^{2+} ions in aqueous solution was labelled with a TAMRA moiety at the 5' end and used as a Raman reporter. Polyamine spermine tetrahydrochloride (spermine) was used to promote surface adsorption of the aptamer probes onto the silver nanoparticles. When Hg^{2+} ions are added to the system, binding of Hg^{2+} with T-T pairs results in a conformational rearrangement of the aptamer to form a hairpin structure. As a result of the reduced of electrostatic repulsion between silver nanoparticles, aggregation of silver nanoparticles occurs, and the SERS signal is significantly increased upon the addition of Hg^{2+} ions. Under optimized assay conditions, the concentration limit of detection was estimated to be 5 nM, and this satisfies a limit of detection below the EPA defined limit of 10 nM in drinkable water

Key Words : Silver nanoparticle, Surface-enhanced raman scattering, Mercury ion, Aptamer sensor

Introduction

Mercury is generally considered to be one of the most toxic environmental pollutants, and is routinely released as a by-product from coal-fired power stations, gold production, oceanic and volcanic emissions and waste disposal.[1,2] In particular, irreversible damage to the central nervous system and other organs are demonstrated results of exposure to high mercury levels in humans of all ages.[3-6] Accordingly, the creation of extremely sensitive and selective techniques for the analysis of mercury (II) ions in environmental, aquatic and food-based environments is of the highest priority. To date, analytical methods, such as atomic absorption spectroscopy (AAS) and inductively coupled plasma-mass spectrometry (ICP-MS), have been shown to provide limits of detection at the parts-per-bilion (ppb) level, but they are costly, time-consuming and unsuited for remote or in-the-field applications.

Alternative approaches based on fluorescence and colorimetric sensing methods have proved promising although most are hindered by relatively poor sensitivity and asscoaited limits-of-detection. Ono and Togashi have recently introduced an aptamer-based sensing system for Hg^{2+} ions in solution.[7] Based on the strong and selective binding of Hg^{2+} ions to thymine-thymine base pairs (T-Hg^{2+}-T) in DNA aptamers, this approach has opened up new possibilities of colorimetric or fluorescent sensing of solvated mercury. Despite such progress, to date few methods have been demonstrated to possess sufficient sensitivity to satisfy the Environmental Protection Agency (EPA) defined maximum contaminant level of 2 ppb (or 10 nM) in drinkable water.[8]

Herein, we demonstrate a highly sensitive surface-enhanced Raman scattering (SERS) platform for the selective sensing of Hg^{2+} ions in aqueous media which is based on the use of structure-folding aptamers on the silver nanoparticles. In recent years, SERS spectroscopy has been shown to be a promising optical technique for high sensitivity analytical detection.[9-11] In particular, due to the ease of synthesizing and functionalizing gold nanoparticles, a range of novel gold nanoparticles modified with entities such as mercaptopropionic acid[12,13] and oligonucleotides[14-18] have been used for mercury sensing. When aptamer molecules are adsorbed onto the surface of silver nanoparticles, they exist as random-coil structures. Upon formation of Hg^{2+}-aptamer complexes, the conformation of the aptamer changes to a hairpin structure.[19-21] This conformational rearrangement of aptamer molecules induces the reduction of electrostatic repulsion between silver nanoparticles. As a result, aggregation of silver nanoparticles occurs, and the SERS signal is significantly increased upon the addition of Hg^{2+} ions. Crucially, the assay is both rapid and simple to implement and yields a concentration detection limit of approximately 5 nM, and this satisfies a limit of detection below the EPA defined limit of 10 nM in drinkable water.

Experimental Section

Silver nanoparticles were prepared by reducing silver nitrate using hydroxoylamine hydrochloride at room temperature.[22] The advantages of the hydroxylamine hydrochloride-reduction are in its speed at room temperature and the fact that produced particles can be used for SERS measurements without further processing. First, 5 mL of 0.03 M hydroxylamine hydrochloride and 1 mL of 0.6 M sodium hydroxide was dissolved in 84 mL of distilled water. Then, 10 mL of 0.01 M silver nitrate was added dropwise to the solution with

vigorous stirring. This solution was continuously stirred for one hour. The prepared silver colloid was stored in a refrigerator at 4 °C before being used. UV/Vis spectroscopy and Transmission Electron Microscopy (TEM) were used to characterize the particle size of the produced colloids, and the average particle size was estimated to be 35 ± 5 nm in diameter. An aptamer (having the sequence 5'-TAMRA-TTCTTTCTTCCCTTGTTTGTT-3') designed to specifically bind to Hg^{2+} ions in aqueous solution was labelled with a carboxytetramethyl-rhodamine (TAMRA) moiety at the 5' end and used as Raman reporter. A random sequence DNA (5'-TAMRA-CGAACCCCCGTGCAGAAAGAA-3') was also prepared for control experiments.

Polyamine spermine tetrahydrochloride (spermine, an organic polyamine) was used to promote surface adsorption of the negatively charged oligonucleotide probe.[23,24] For spermine optimization, 1 μL of 10 μM TAMRA-labelled aptamer was pre-mixed with 5 μL of 100 μM spermine. This solution was then mixed with 200 μL of silver nanocolloids. Finally, various concentrations of $Hg(NO_3)_2$ solution were prepared and added to each aptamer-conjugated silver nanocolloid and incubated for 3 min.

SERS measurements were performed using a Renishaw 2000 Raman microscope system, with a Melles Griot He-Ne laser operating at a wavelength 632.8 nm and a power of 12 mW. The Rayleigh line was removed from the collected Raman signal using a holographic notch filter located in the collection path. Raman scattering was measured using a charge-coupled device (CCD) camera with a spectral resolution of 4 cm^{-1}. UV/Vis absorption measurements were performed using a Varian Cary 100 UV/vis spectrophotometer. TEM images were obtained using a Hitachi H-700 transmission microscope.

Results and Discussion

Figure 1(a) depicts the mechanism of a mercury ion detection using a mercury specific aptamer. A specifically designed aptamer presents a random-coil structure in the absence of Hg^{2+} ions but it forms hairpin structure in the presence of Hg^{2+} ions. It is because the T-T mismatch shows a high sensitivity to Hg^{2+} ion against other metal ions. Here, Raman reporter, TAMRA was attached at the 5' terminus for SERS measurements. Figure 1(b) illustrates the basic concept of mercury 'signal-on' detection using structure-switching aptamer-conjugated silver nanoparticles. Bare silver nanoparticles are well dispersed after synthesis because they are stabilized by negatively charged hydroxyl amine chloride

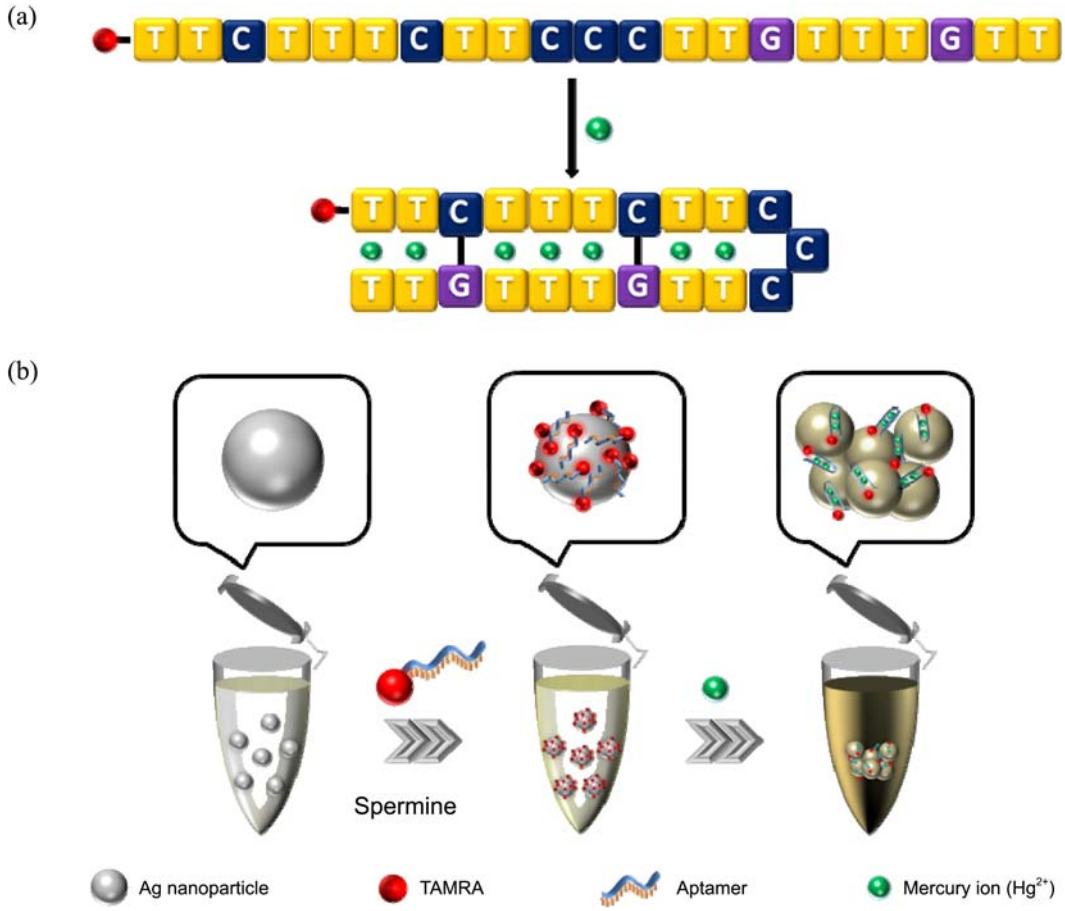

Figure 1. (a) Mechanism of a mercury detection using a specifically designed structure-switching aptamer. Upon formation of Hg^{2+}-aptamer complexes, the conformation of the aptamer changes to a hairpin structure. (b) Working principle of the SERS-based Hg^{2+} aptameric sensor. When Hg^{2+} ions are added to the system together with spermine, binding of Hg^{2+} with T-T pairs results in a conformational rearrangement of the aptamer to form a hairpin structure. This conformational change causes a particle aggregation between silver nanoparticles.

ions coating their surface. The addition of spermine aids efficient adsorption of aptamer molecules onto the silver nanoparticle surface, since the spermine acts as a bridge between the two negatively charged species and also reduces the net surface negative charge on the silver surface. Thus, aptamer molecules effectively adsorb onto the surface of silver nanoparticles through electrostatic attraction. In the presence of spermine, however, the ss-DNA aptamer molecule on the surface of silver nanoparticles keeps a random-coil structure as a result of electrostatic repulsion between DNA molecules. If Hg^{2+} ions are now added to the system, binding of Hg^{2+} with T-T pairs results in a conformational rearrangement of the aptamer to form a hairpin structure. This conformational change causes a further reduction in electrostatic repulsion and when combined with steric stabilization a drastic increase in particle aggregation is observed. In other words, the conformation of ss-DNA changes to folded structures by the formation of Hg^{2+}-DNA complexes in the presence of Hg^{2+} ions. As a result, the negative charge intensity of folded DNA is dereased and the reduced degree of electrostatic repulsion between silver nanoparticles induces particle aggregations. Three different protocols, using the particle aggregation caused by structure-switching aptamer-conjugated metal nanoparticles, have been reported for Hg^{2+} detection. One is the fluorescence resonance energy transfer between fluorescein and dabcyl which are labeled on both ends of an aptamer.[7,24] Here, the hairpin formation leads them to come to close proximity to quenching. The other two protocols are based on the changes of UV/vis absorption[16,17,25] or fluorescence emission[26] along the Hg^{2+}-induced aggregation of aptamer-conjugated metal nanoparticles. All three protocols have shown a high selectivity for Hg^{2+} ions but their sensitivity is still far from the EPA defined maximum contaminant level of 2 ppb (or 10 nM) in drinkable water.[8]

Key idea to the current sensing method is the fact that nanoparticle aggregates provide excellent signal enhancement of Raman peaks from the TAMRA reporters. This great enhancement is caused by the large electromagnetic field produced by hot spots, which resides in the nanoscale junctions in metal nanostructures such as dimers or aggregates. According to recent SERS data reported by Kneipp *et al.*,[27] the SERS enhancement factor for silver nanoclusters found to be seven orders of magnitude higher than the enhancement factor for isolated silver nanoparticles. Accordingly, the recovered SERS signal is significantly increased upon the particle aggregation caused by the addition of Hg^{2+} ions, and it is expected to be more sensitive than absorption or fluorescence dection method.

The Hg^{2+} ion-induced aggregation of the silver nanoparticles was directly supported by TEM images. Figure 2 presents the TEM images and corresponding SERS spectra that reveal (a) bare silver nanoparticles in the absence of Hg^{2+} ions and (b) their aggregations in the presence of 5 μM of Hg^{2+} ions (b). Here, the visual detection of the presence of Hg^{2+} ions is also possible since the color of the colloid solution has been changed from yellow to green upon the addition of Hg^{2+} ions. Nonetheless, SERS detections along different concentrations of Hg^{2+} ions have been performed for their highly sensitive trace analysis. We also conducted control experiments using a random sequence DNA (5'-TAMRA-CGAACCCCCGTGCAGAAAGAA-3') under similar conditions. As expected, the addition of Hg^{2+} ions did not induce any significant changes in SERS spectra.

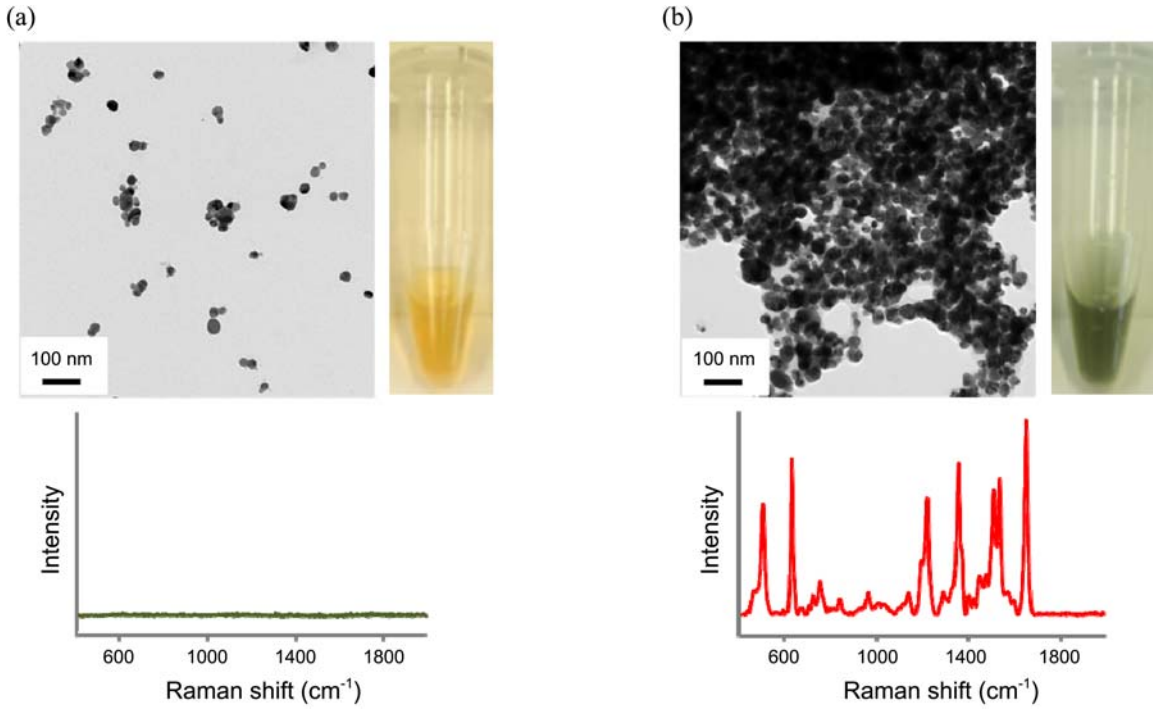

Figure 2. TEM images, visual color changes, and SERS spectra corresponding to (a) non-aggregated bare silver nanoparticles and (b) aggregated nanoparticles after adding 5 μM Hg^{2+} in the presence of 10 μM TAMRA-labelled aptamer and 100 μM spermine.

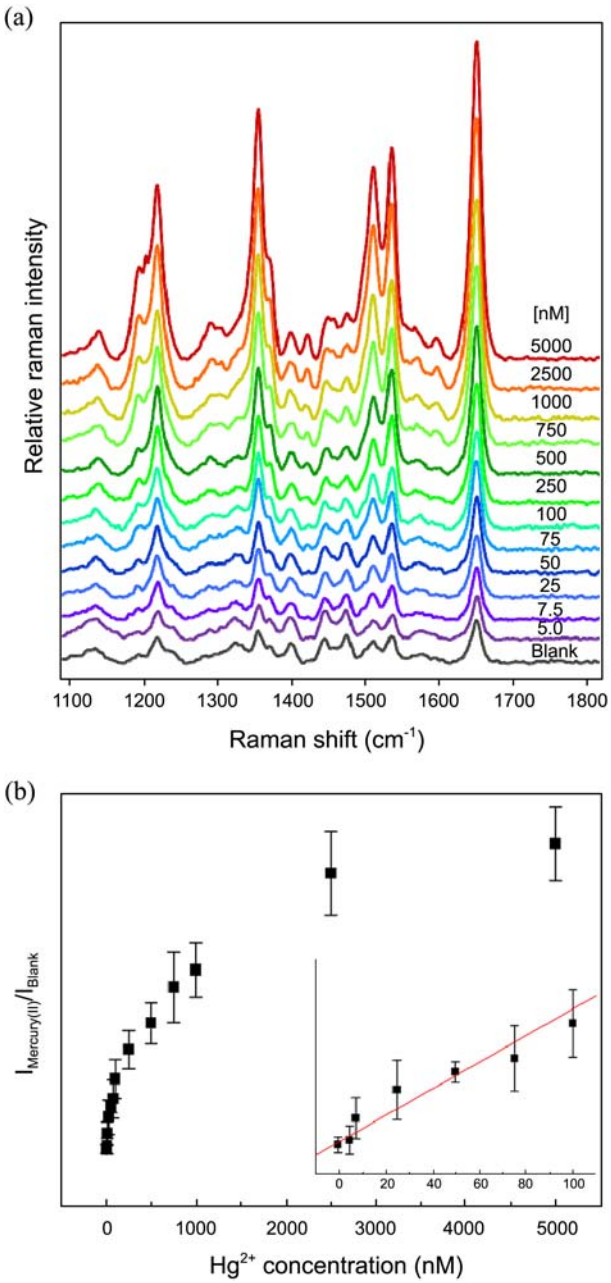

Figure 3. (a) SERS spectra changes upon the addition of various amount of Hg^{2+} and (b) plots of corresponding intensity ratio ($I_{Mercury(II)}/I_{Blank}$) of the Raman band centered at 1651 cm^{-1} as a function of Hg^{2+} concentration. Insert shows a linear relationship in the lower concentration range from 0 to 100 nM (R=0.982). Error bars indicate standard deviations from three measurements.

Figure 3(a) presents measured SERS spectra of aptamer-conjugated silver nanoparticles as a function of Hg^{2+} ion concentration and at the optimum spermine concentration. The strongest Raman peaks for TAMRA are observed at 1650, 1534, 1512, 1356 and 1217 cm^{-1}. It can be seen that average SERS intensities for all peaks increase as a function of Hg^{2+} ion concentration. This relationship is expounded in Figure 3(b) where the variation in the intensity of the 1651 cm^{-1} TAMRA peak is plotted as a function of Hg^{2+} ion concentration. These data were analysed using the following non-linear regression model.

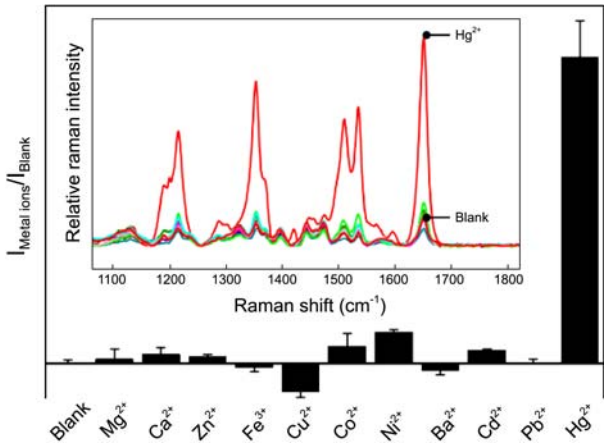

Figure 4. Metal ion-induced SERS intensity changes of proposed Hg^{2+} SERS sensor. Insert shows the SERS spectra changes upon kinds of metal ions. All the metal ion concentrations are 5.0 μM. Error bars indicate standard deviations from three measurements.

$$S = 1 + S_{MAX} \cdot \frac{[Hg^{2+}]}{[Hg^{2+}] + K}$$

Here S defines the intensity ratio of $I_{Mercury(II)}/I_{Blank}$, K is the fitting parameter and $[Hg^{2+}]$ is the concentration of the Hg^{2+} in solution. Such a non-linear fit of the data yields K = 728 nM and S_{MAX} = 5.94. It should also be noted that further analysis using a Hill model (data not shown) was performed to determine cooperativity in the binding mercury ions to the aptamer.[28] This analysis was inconclusive (yielding a Hill coefficient of 0.5) and forbade conclusions to be made regarding cooperativity. It can be seen (inset of Fig. 3(b)) that good linearity is observed for Hg^{2+} concentrations up to 100 nM (R=0.982). Additionally, the concentration limit of detection (based on a minimum signal-to-noise ratio of 3) was calculated to be 5 nM. This confirms the exquisite sensitivity of the assay, which is two orders of magnitude lower than reported for other heavy metal ion sensing techniques, and more importantly yields a limit of detection below the EPA defined limit of 10 nM in drinkable water.[8]

Under optimised conditions, we investigated the selectivity of our approach towards Hg^{2+} ions against ten other metal ions (each at a concentration of 5.0 μM). As can been in Figure 4, only the addition of Hg^{2+} ions leads to a signficant increase in the SERS signal. This indicates that only Hg^{2+} ions induced aggregation of the silver nanoparticles in the presence of specifically designed aptamers. We tested a range of metal ions including alkaline earths (Mg^{2+}, Ca^{2+} and Ba^{2+}) and transition heavy metal ions (Zn^{2+}, Fe^{3+}, Cu^{2+}, Co^{2+}, Ni^{2+}, Cd^{2+} and Pb^{2+}). The highest SERS response is consistent with the much high affinity of the designed aptamer towards aqueous Hg^{2+} ions.

Conclusions

In the present work, we have successfully demonstrated a

highly sensitive and selective method for the detection of Hg^{2+} ions in aqueous media. Several different absorption- or fluorescence-based detection protocols, using the particle aggregation caused by structure-switching aptamer-conjugated metal nanoparticles, have been previously reported for Hg^{2+} detection. However, the detection sensitivity is still far above the EPA defined toxic level of Hg^{2+} ions of 10 nM in drinkable water. Herein, we successfully developed a simple T-Hg^{2+}-T based SERS detection method for the first time. By leveraging the strong affinity between Hg^{2+} ions and thymine-thymine base pairs, changes in the SERS signals of TMARA molecules were successful in reporting Hg^{2+} ion concentration down to 5 nM. Moreover, since Raman reporters have distinct and resolvable Raman fingerprints, such SERS-based aptameric sensors have a tremendous capacity for multiplexed assays.

Acknowledgments. This work was supported by the National Research Foundation of Korea (Grant Numbers R11-2011-044-1002-0 and K20904000004-09A050000410), and the KRIBB Research Initiative Program. This work was also partially supported by the GRRC Program of Gyeonggi Province (GRRC-Hanyang-2010-CO3, USN for Plant Factory).

References

1. Campbell, L. M.; Dixon, D.G.; Hecky, R. E. *J. Toxicol. Environ. Health B* **2003**, *6*, 325-356.
2. Sekowski, J. K.; Malkas, L. H.; Wei, Y.; Hickey, R. J. *Toxicol. Appl. Pharmacol.* **1997**, *145*, 268-276.
3. Onyido, I.; Noris, A. R.; Buncel, E. *Chem. Rev.* **2004**, *104*, 5911-5929.
4. Reardon, A. M.; Bhat, H. K. *Toxicol. Environ. Chem.* **2007**, *89*, 535-554.
5. Yin, Z.; Milatovic, D.; Aschner, J. L.; Synersen, T.; Rocha, J. B. T.; Souza, D. O.; Sidoryk, M.; Albrecht, J.; Aschner, M. *Brain Res.* **2007**, *1131*, 1-10.
6. Tamm, C.; Duckworth, J.; Hermanson, O.; Ceccatelli, S. *Neurochem, J.* **2006**, *97*, 69-78.
7. Ono, A.; Togashi, H. *Angew. Chem. Int. Ed.* **2004**, *116*, 4300-4302.
8. US EPA (2001), Mercury update: impact on fish advisories, EPA-823-F-01-011.
9. Nie, S. M.; Emery, S. R. *Science* **1997**, *275*, 1102-1106.
10. Tian, Z. Q.; Ren, B.; Wu, D. Y. *J. Phys. Chem. B* **2002**, *106*, 9463-9483.
11. Huang, C. C.; Chang, H. T. *Chem. Commun.* **2007**, 1215-1217.
12. Wang, G.; Lim, C.; Chen, L.; Chon, H.; Choo, J.; Hong, J.; deMello, A. J. *Anal. Bioanal. Chem.* **2009**, *394*, 1827-1832.
13. Yu, C. J.; Tseng, W. L. *Langmuir* **2008**, *24*, 12717-12722.
14. Lee, J. S.; Han, M. S.; Mirkin, C. A. *Angew. Chem. Int. Ed.* **2007**, *46*, 4093-4096.
15. Liu, C. W.; Hsieh, Y. T.; Huang, C. C.; Lin, Z. H.; Chang, H. T. *Chem. Commun.* **2008**, 2242-2244.
16. Liu, C. W.; Huang, C. C.; Chang, H. T. *Langmuir* **2008**, *24*, 8346-8350.
17. Li, D.; Wieckowska, D.; Willner, I. *Angew. Chem., Int. Ed.* **2008**, *46*, 4093-4096.
18. Lee, J. S.; Lytton-Jean, A. K. R.; Mirkin, C. A. *Nano Lett.* **2007**, *7*, 2112-2115.
19. Wang, Z.; Lee, J. H.; Lu, Y. *Chem. Commun.* **2008**, 6005-6007.
20. Zhao, W.; Chiuman, W.; Lam, J. C. F.; McManus, S. A.; Chen, W.; Cui, Y.; Pelton, R.; Brook, M. A.; Li, Y. J. *J. Am. Chem. Soc.* **2008**, *130*, 3610-3618.
21. Wang, G.; Chen, L. *Chinese Chem. Lett.* **2009**, *20*, 1475-1477.
22. Leopold, N.; Lendl, B. *J. Phys. Chem. B* **2003**, *107*, 5723-5727.
23. Jones, J. C.; McLaughlin, C.; Littlejohn, D.; Sadler, D. A.; Graham, D.; Smith, W. E. *Anal. Chem.* **1999**, *71*, 596-601.
24. Graham, D.; Faulds, K. *Chem. Soc. Rev.* **2008**, *37*, 1042-1051.
25. Chiang, C. K.; Huang, C. C.; Liu, C. W.; Chang, H. T. *Anal. Chem.* **2008**, *80*, 3716-3721.
26. Wang, J.; Liu, B. *Chem. Commun.* **2008**, 4759-4761.
27. Kneipp, K.; Kneipp, H.; Kneipp, J. *Acc. Chem. Res.* **2006**, *39*, 443-450.
28. Srisa-Art, M.; Kang, D. K.; Hong, J.; Park, H.; Leatherbarrow, R. J.; Edel, J.B.; Chang, S. I.; deMello, A. J. *ChemBioChem* **2009**, *10*, 1605-1611.